Burial and scour of truncated cones due to long-crested and short-crested nonlinear random waves

Dag Myrhaug[*1] and Muk Chen Ong[2]

[1]*Department of Marine Technology, Norwegian University of Science and Technology, NO-7491 Trondheim, Norway*
[2]*Norwegian Marine Technology Research Institute (MARINTEK), NO-7450 Trondheim, Norway*

Abstract. This paper provides a practical stochastic method by which the burial and scour depths of truncated cones exposed to long-crested (2D) and short-crested (3D) nonlinear random waves can be derived. The approach is based on assuming the waves to be a stationary narrow-band random process, adopting the Forristall (2000) wave crest height distribution representing both 2D and 3D nonlinear random waves. Moreover, the formulas for the burial and the scour depths for regular waves presented by Catano-Lopera *et al*. (2011) for truncated cones are used. An example of calculation is also presented.

Keywords: burial; scour; truncated cones; long-crested waves; short-crested waves; nonlinear random waves; stochastic approach

1. Introduction

The present work addresses the burial and scour of truncated cones beneath random waves including effects of second order wave asymmetry. Typical examples of truncated cones in such environments are sea mines on the seabed. Such bodies, which originally were installed, e.g., on a plane bed, may experience a range of seabed conditions, i.e., the bed may be flat or rippled; they may be surrounded by a scour hole, and they may be self-buried. This is caused by the complicated three-dimensional flow generated by the interaction between the incoming flow velocity (e.g., the relative magnitude between waves and current), the geometry of the bed, the bed material, the ratio between the near-bed oscillatory fluid particle excursion amplitude and the characteristic dimensions of the body. Moreover, real waves are stochastic, making the problem more complex.

Further details on the general background and complexity of scour in the marine environment, as well as reviews of the problems are given in, e.g., Whitehouse (1998) and Sumer and Fredsøe (2002). To our knowledge, no studies are available in the open literature dealing with random wave burial and scour of truncated cones. The specifics related to scour around truncated cones as well as self-burial of such bodies exposed to steady currents and regular waves are addressed in Catano-Lopera *et al*. (2011). Catano-Lopera *et al*. (2011) carried out laboratory tests studying systematically the burial and scour of truncated cones. Examples of other studies are numerical

---

*Corresponding author, Professor, E-mail: dag.myrhaug@ntnu.no

modelling (Jenkins *et al.* 2007) and field investigations (Guyonic *et al.* 2007, Mayer *et al.* 2007). Catano-Lopera *et al.* (2011) also gave a review of other works related to truncated cones.

The purpose of this paper is to present a practical approach by which the burial and scour of truncated cones in nonlinear random waves can be derived. Here the empirical formulas based on data from laboratory tests for regular waves presented by Catano-Lopera *et al.* (2011) are used.

The approach is based on assuming the waves to be a stationary narrow-band process, and adopting the Forristall (2000) wave crest height distribution representing both long-crested (2D) and short-crested (3D) nonlinear random waves. Examples of calculation are also given to demonstrate the application of the method.

A review of the present stochastic method is given in Myrhaug and Ong (2011a). This stochastic method has recently been extended to provide a practical method for the scour due to 2D and 3D nonlinear random waves; below pipelines (Myrhaug and Ong 2011b); below spherical bodies (Myrhaug and Ong 2012); around vertical piles (Myrhaug and Ong 2013 a, b, Ong *et al.* 2013); burial and scour of short cylinders (Myrhaug *et al.* 2012).
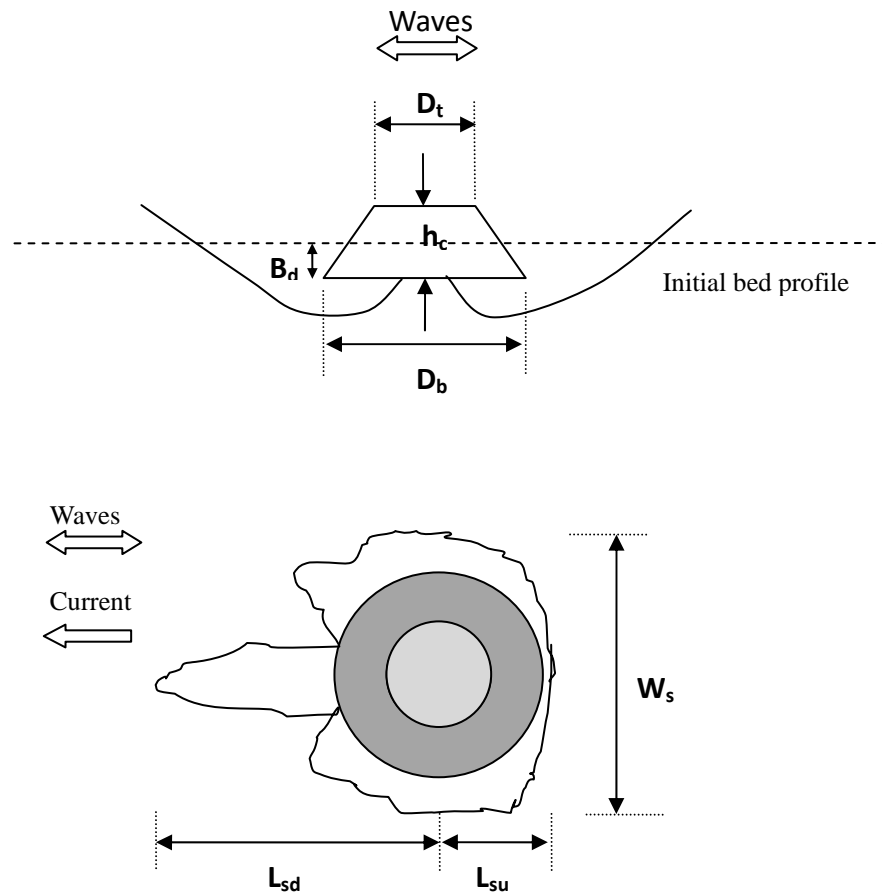

Fig. 1 Definition sketch of the burial depth (B_d), the scour width (W_s), and the scour length (L_{sd}, L_{su}) of the scour hole around a truncated cone (reproduced from Catano-Lopera *et al.* 2011)

2. Burial and scour in regular waves

2.1 Burial of truncated cones

The burial of conical frustums, or truncated cones (hereafter referred to as cones) under combined regular waves and currents was investigated in laboratory tests by Catano-Lopera *et al.* (2011). For waves alone they obtained the following empirical formula for the equilibrium relative burial depth B_d of the cone with height h_c, base diameter D_b and top diameter D_t, with $D_t / D_b = 0.5$ (see Fig. 1)

$$\frac{B_d}{h_c} = pKC^r\theta^s \; ; (p, r, s) = (0.0125, 0.8, 0.1) \tag{1}$$

Here U is the undisturbed linear near-bed orbital velocity amplitude, and KC is the Keulegan-Carpenter number defined by

$$KC = \frac{UT}{D} \tag{2}$$

where T is the wave period, and D is a representative diameter, defined as the average, i.e., $D = (D_b + D_t)/2$. Eq. (1) is valid for live-bed scour, for which $\theta > \theta_{cr}$, where θ is the undisturbed Shields parameter defined by

$$\theta = \frac{\tau_w}{\rho g(\gamma - 1)d_{50}} \tag{3}$$

where τ_w is the maximum bottom shear stress under waves, ρ is the density of the fluid, g is the acceleration due to gravity, $\gamma = \rho_s / \rho$ is the sediment grain density to fluid density ratio, ρ_s is the sediment grain density, d_{50} is the median grain size diameter, and θ_{cr} is the critical value of motion at the bed, i.e., $\theta_{cr} \approx 0.05$. One should note that the scour process attains its equilibrium stage through a transition period. Thus the approach is valid when it is assumed that the storm has lasted longer than the time scale of the scour.

The main mechanism of the burial and scour process of a truncated cone were observed and described by Catano-Lopera *et al.* (2011). The major flow structures that cause the burial and scour around the truncated cone placed on the seabed are the complicated flow patterns surrounding the cone due to the back and forth motion of the waves governed by *KC*. During the first half wave cycle the flow field around a cone is characterized by a combination of upstream horseshoe vortices, streamline contractions around and over the cone, and vortex shedding in the wake. The vortex shedding brings the sediments into suspension carrying them away from the cone, and transported away by the outer flow. During the second half wave cycle the situation is reversed, and consequently the sediments are transported opposite to the wave propagation direction. For nonlinear waves the flow structures have higher intensity in the wave propagation direction due to asymmetry in the wave shape. More details are given in Catano-Lopera *et al.* (2011).

The maximum bottom shear stress within a wave cycle is taken as

$$\frac{\tau_w}{\rho} = \frac{1}{2} f_w U^2 \qquad (4)$$

where f_w is the friction factor, which here is taken from Myrhaug *et al.* (2001), valid for waves plus current for wave-dominant situations (see Myrhaug *et al.* 2001, Table 3)

$$f_w = c \left(\frac{A}{z_0} \right)^{-d} \qquad (5)$$

$$(c, d) = (18, 1) \text{ for } 20 \le A / z_0 \le 200 \qquad (6)$$

$$(c, d) = (1.39, 0.52) \text{ for } 200 \le A / z_0 \le 11000 \qquad (7)$$

$$(c, d) = (0.112, 0.25) \text{ for } 11000 \le A / z_0 \qquad (8)$$

where $A = U / \omega$ is the near-bed orbital displacement amplitude, $\omega = 2\pi / T$ is the angular wave frequency, and $z_o = d_{50}/12$ is the bed roughness. The advantage of using this friction factor for rough turbulent flow is that it is possible to derive the stochastic approach analytically. Note that Eq. (7) corresponds to the coefficient given by Soulsby (1997) obtained as best fit to data for $10 \le A / z_0 \le 10^5$.

One should notice that the KC number can alternatively be expressed as

$$KC = \frac{2\pi A}{D} \qquad (9)$$

Moreover, *A* is related to the linear wave amplitude *a* by

$$A = \frac{a}{\sinh kh} \qquad (10)$$

where *h* is the water depth, and *k* is the wave number determined from the dispersion relationship $\omega^2 = gk \tanh kh$.

Eq. (1) is based on data for which $1.5 \le KC \le 16$ and $0.04 \le \theta \le 0.34$. It should be noted that since Eq. (1) appears to be physically sound for $KC > 0$, i.e., B_d equals zero for $KC = 0$, the formula can be taken to be valid from $KC = 0$. This extension of Eq. (1) relies on the threshold of sediment motion to be exceeded, which for small values of *KC* may not be the case.

2.2 Scour around truncated cones

The scour around a cone in regular waves plus currents was investigated in laboratory tests by Catano-Lopera *et al.* (2011). They obtained the following empirical formulas for the geometric dimensions of the scour hole; the scour hole width W_s, the relative downstream length L_{sd}, and the total scour hole length L_{st} (see Fig. 1)

$$\frac{W_s}{D} = pKC^r \theta^s \ ; \ (p, r, s) = (1.03, 0.1, 0.05) \qquad (11)$$

$$\frac{L}{D} = pKC^r \tag{12}$$

where L represents L_{sd} and L_{st}. For the following representations of L the coefficients p and r are given as

$$L = L_{sd} \ ; \ (p,r) = (0.43, 0.46) \tag{13}$$

$$L = L_{st} \ ; \ (p,r) = (0.80, 0.34) \tag{14}$$

Then the relative upstream length of the scour hole is given as $L_{su} = L_{st} - L_{sd}$. Eqs. (11) to (14) are valid for the same conditions as described in Section 2.1.

The sinking of the cone is primarily caused by the combination of the tunnelling underneath the cone and the continuous reduction of the span shoulder, which is located underneath the centre of the cone and is reduced towards the center. As the scour develops, the bearing capacity of the soil will be exceeded, causing the soil to fail; the cone will sink. The whole process will continue until the failure of the soil stops, and subsequently the sinking ends. More details about the mechanisms and the time evolution of the process are described in Catalano *et al.* (2011).

2.3 Summary of burial and scour of truncated cones

The results presented in Sections 2.1 and 2.2 can be summarized and is presented in Table 1. All the formulas can be represented by

$$\frac{Y}{D} = pKC^r \theta^s \tag{15}$$

where p,r,s are given in Table 1 for the different responses Y and the object dimensions D.

3. Burial and scour in nonlinear random waves

3.1 Theoretical background

Under nonlinear waves the nonlinearity is primarily caused by the asymmetric wave velocity, i.e., that the near-bed orbital velocity is larger in the wave propagation direction than in the opposite direction. Catano-Lopera and Garcia (2007) addressed the effect of wave asymmetry on the scour depth around a finite length cylinder placed horizontally on a plane bed. In their experiments in regular waves plus currents they observed that normally the downstream length of the scour gap is larger than its upstream counterpart. Under waves alone this is primarily caused by the asymmetric wave velocity. Examples of wave asymmetry are shown in their Figs. 2(b) and 3(b). However, the effect of this asymmetry on the geometry of the scour hole was not elaborated further. In the present paper the effects of wave asymmetry are considered by using Stokes second-order wave theory.

Table 1 Summary of the scour responses Y and the object dimensions D for waves alone and the coefficients in Eq. (15) as well as the coefficient t in Eqs. (34) to (37)

Y	D	p	r	s	t
B_d	h_c	0.0125	0.8	0.1	0.975
W_s	$(D_b+D_t)/2$	1.03	0.1	0.05	0.1875
L_{sd}	$(D_b+D_t)/2$	0.43	0.46	0	0.46
L_{st}	$(D_b+D_t)/2$	0.80	0.34	0	0.34

For Stokes second-order waves the nonlinearity is primarily caused by the larger velocity under the wave crest (crest velocity) than under the wave trough (trough velocity). Based on the results by Catano-Lopera and Garcia (2007) referred to earlier, it seems that it is the largest velocity in the wave cycle (i.e., the crest velocity) which is responsible for the scour, rather than the mean of the crest velocity and the trough velocity (i.e., equal to the linear wave velocity). Thus the scour response characteristics for individual random Stokes second-order waves are obtained from Eq. (15) by replacing U with U_m, i.e., the maximum near-bed orbital velocity under the wave crest. This will be elaborated upon further in the forthcoming section.

At a fixed point in a sea state with stationary narrow-band random waves consistent with Stokes second-order regular waves in finite water depth h, the non-dimensional nonlinear crest height, $w_c = \eta_c / a_{rms}$, and the non-dimensional nonlinear maximum horizontal particle velocity evaluated at the seabed, $\hat{U}_m = U_m / U_{rms}$, are (Dean and Dalrymple 1984)

$$w_c = \hat{a} + O\left(k_p a_{rms}\right) \tag{16}$$

$$\hat{U}_m = \hat{a} + O\left(k_p a_{rms}\right) \tag{17}$$

Here $\hat{a} = a / a_{rms}$ is the non-dimensional linear wave amplitude, where the linear wave amplitude a is made dimensionless with the *rms* (root-mean-square) value a_{rms}, and

$$U_{rms} = \frac{\omega_p a_{rms}}{\sinh k_p h} \tag{18}$$

Moreover, $O\left(k_p a_{rms}\right)$ denotes the second-order (nonlinear) terms which are proportional to the characteristic wave steepness of the sea state, $k_p a_{rms}$, where k_p is the wave number corresponding to ω_p (the peak frequency of the wave spectrum) given by the dispersion relationship for linear waves (which is also valid for Stokes second-order waves)

$$\omega_p^2 = g k_p \tanh k_p h \tag{19}$$

Now Eq. (16) can be inverted to give $\hat{a} = w_c - O\left(k_p a_{rms}\right)$, which substituted in Eq. (17) gives

$\hat{U}_m = w_c + O\left(k_p a_{rms}\right)$. Thus it appears that $\hat{a}$ can be replaced by w_c in the linear term of $\hat{U}_m$, because the error involved is of second order. Consequently, by neglecting terms of $O\left(k_p a_{rms}\right)$ the maximum near-bed orbital velocity under the wave crest in dimensional form can be taken as

$$U_m = \frac{\omega_p \eta_c}{\sinh k_p h} \tag{20}$$

Moreover, $A_m = U_m / \omega_p$ is the maximum near-bed orbital displacement under the wave crest, $\hat{A}_m = A_m / A_{rms}$ is the non-dimensional maximum near-bed orbital displacement where

$$A_{rms} = \frac{a_{rms}}{\sinh k_p h} \tag{21}$$

Furthermore

$$\omega_p = \frac{U_m}{A_m} = \frac{U_{rms}}{A_{rms}} \tag{22}$$

by combining Eqs. (18) and (21).

Now the Forristall (2000) parametric crest height distribution based on simulations using second-order theory is adopted. The simulations were based on the Sharma and Dean (1981) theory; this model includes both sum-frequency and difference-frequency effects. The simulations were made both for 2D and 3D random waves. A two-parameter Weibull distribution with the cumulative distribution function (*cdf*) of the form

$$P\left(w_c\right) = 1 - \exp\left[-\left(\frac{w_c}{\sqrt{8}\alpha}\right)^\beta\right] \ ; \ w_c \geq 0 \tag{23}$$

was fitted to the simulated wave data. The Weibull parameters α and β were estimated from the fit to the simulated wave data and are based on the wave steepness S_1 and the Ursell parameter U_R defined by

$$S_1 = \frac{2\pi}{g} \frac{H_s}{T_1^2} \tag{24}$$

and

$$U_R = \frac{H_s}{k_1^2 h^3} \tag{25}$$

Here H_s is the significant wave height, T_1 is the spectral mean wave period, and k_1 is the wave number corresponding to T_1. It should be noted that $H_s = 2\sqrt{2}a_{rms}$ when a is Rayleigh distributed. The wave steepness and the Ursell number characterize the degree of nonlinearity of the random waves in finite water depth. At zero steepness and zero Ursell number the fits were forced to match

the Rayleigh distribution, i.e., $\alpha = 1/\sqrt{8} \approx 0.3536$ and $\beta = 2$. Note that this is the case for both 2D and 3D linear waves. The resulting parameters for the 2D-model are

$$\alpha_{2D} = 0.3536 + 0.2892S_1 + 0.1060U_R$$
$$\beta_{2D} = 2 - 2.1597S_1 + 0.0968U_R^2 \tag{26}$$

and for the 3D-model

$$\alpha_{3D} = 0.3536 + 0.2568S_1 + 0.0800U_R$$
$$\beta_{3D} = 2 - 1.7912S_1 - 0.5302U_R + 0.284U_R^2 \tag{27}$$

Forristall (2000) demonstrated that the wave setdown effects were smaller for short-crested than for long-crested waves, which is due to the fact that the second-order negative difference-frequency terms are smaller for 3D waves than for 2D waves. Consequently the wave crest heights are larger for 3D waves than for 2D waves.

3.2 Outline of stochastic method

For scour below pipelines and around vertical piles in random waves Sumer and Fredsøe (1996, 2001) determined the statistical quantities of wave height H and wave period T to be used in the regular wave formulas for the scour depth and the scour width below pipelines and the scour depth around slender vertical piles. By trial and error they found that the use of H_{rms} (*rms* wave height) and T_P (peak period of the wave spectrum) gave the best agreement with data. Here a tentative stochastic approach will be outlined. The highest among random waves in a stationary narrow-band sea-state is considered, as it is reasonable to assume that it is mainly the highest waves which are responsible for the scour response. It is also assumed that the sea-state has lasted long enough to develop the equilibrium scour depth. The highest waves considered here are those exceeding the probability $1/n$, $w_{c1/n}$ (i.e., $1 - P(w_{c1/n}) = 1/n$). The parameter of interest is the expected (mean) of the maximum equilibrium scour characteristics caused by the $(1/n)$ th highest wave crests, which is given as

$$E[Y(w_c)/w_c > w_{c1/n}] = n \int_{w_{c1/n}}^{\infty} Y(w_c)p(w_c)dw_c \tag{28}$$

where Y represents the scour characteristics, and $p(w_c)$ is the probability density function (*pdf*) of w_c. More specifically, the present approach is based on the following assumptions: (1) the free surface elevation is a stationary narrow-band process with zero expectation, and (2) the scour response formulas for regular waves plus current given in the previous section (Eq. (15)), are valid for irregular waves as well. These assumptions are essentially the same as those given in e.g. Myrhaug *et al.* (2009), where further details are found.

For a narrow-band process $T = T_p$ where $T_p = 2\pi/\omega_p = 2\pi A_{rms}/U_{rms}$ and where Eq. (22) has been used. By taking $U = U_m$, $A = A_m$ and substituting this in Eq. (15) using Eqs. (2) to (5), and using from Eq. (22) that $A_m/A_{rms} = U_m/U_{rms}$, Eq. (15) can be re-arranged to give the scour

characteristics by individual narrow-band nonlinear random waves as (and using that $\hat{U}_m = w_c$ by neglecting terms of $O(k_p a_{rms})$)

$$y \equiv \frac{Y/D}{pKC_{rms}^r \theta_{rms}^s} = w_c^{r+s(2-d)} \tag{29}$$

where

$$KC_{rms} = \frac{U_{rms}T_p}{D} = \frac{2\pi A_{rms}}{D} \tag{30}$$

$$\theta_{rms} \frac{\frac{1}{2}c\left(\frac{A_{rms}}{z_0}\right)^{-d} U^2_{rms}}{g(\gamma-1)d_{50}} \tag{31}$$

It should be noted that KC_{rms} and θ_{rms} are uniquely defined for given values of U_{rms}, A_{rms} and T_p.

Now the mean of the maximum scour characteristics caused by the $(1/n)$th highest wave crests follows from Eqs. (28) and (29) as

$$E\left[y(w_c) \mid w_c > w_{c1/n}\right] = n \int_{w_{c1/n}}^{\infty} w_c^{r+s(2-d)} p(w_c)dw_c \tag{32}$$

where $p(w_c) = dP(w_c)/dw_c$ with $P(w_c)$ as given in Eq. (23), and by using that

$$w_{c1/n} = \sqrt{8}\alpha\left(\ln n\right)^{1/\beta} \tag{33}$$

The result is (see the Appendix)

$$E\left[y(w_c) \mid w_c > w_{c1/n}\right] = n\left(\sqrt{8}\alpha\right)^t \Gamma\left(1+\frac{t}{\beta}, \ln n\right) \; ; \; t = r + s(2-d) \tag{34}$$

where $\Gamma(\cdot,\cdot)$ is the incomplete gamma function.

The results for linear waves ($\alpha = 1/\sqrt{8}, \beta = 2$), are obtained from Eq. (34) as

$$E\left[y(w_c) \mid w_c > w_{c1/n}\right] = n\Gamma\left(1+\frac{t}{2}, \ln n\right) \; ; \; t = r + s(2-d) \tag{35}$$

4. Results and discussion

For random wave-induced scour around cones due to 2D and 3D nonlinear waves no data

currently exist in the open literature. Therefore, the results in this section should be taken as tentative, and data for comparisons are required before any conclusion can be made regarding the validity of the approach. A recent review of the authors' previous studies on random wave-induced equilibrium scour characteristics around marine structures including comparison with data from random wave-induced scour experiments is given in Myrhaug and Ong (2011a). This supports that the method should be useful as an engineering approach.

First, the main results are presented. Second, the appropriate Shields parameter to use to determine the conditions corresponding to live-bed scour for 2D and 3D nonlinear random waves is discussed. Third, an example is given to demonstrate the use of the method. Finally, a brief discussion of the results is provided.

4.1 Main results

A feature of interest is to compare the nonlinear results in Eq. (34) with the corresponding linear results for both 2D and 3D waves in Eq. (35).

For waves alone, the nonlinear to linear ratio based on Eqs. (34) and (35) is obtained as

$$R_1 = \left(\sqrt{8}\alpha\right)^t \frac{\Gamma\left(1+\dfrac{t}{\beta},\ln n\right)}{\Gamma\left(1+\dfrac{t}{2},\ln n\right)}; \quad t = r + s(2-d) \tag{36}$$

Another interesting feature is to compare the 3D and 2D results. The ratio between the maximum equilibrium scour characteristics for 3D waves and the maximum equilibrium scour characteristics for 2D waves based on Eq. (34) is obtained as

$$R_2 = \left(\frac{\alpha_{3D}}{\alpha_{2D}}\right)^t \frac{\Gamma\left(1+\dfrac{t}{\beta_{3D}},\ln n\right)}{\Gamma\left(1+\dfrac{t}{\beta_{2D}},\ln n\right)}; \quad t = r + s(2-d) \tag{37}$$

It should be noted that R_1 and R_2 are both independent of KC_{rms}; only dependent of S_1 and U_R.

The results are exemplified by calculating the ratios R_1 and R_2 for the equilibrium burial depth B_d, i.e., using the results for $r = 0.8$, $s = 0.1$ (see Eq. (1) and Table 1) and $d = 0.25$ (see Eqs. (5) and (8)). The results for the other scour characteristics, i.e. W_s, L_{sd}, L_{st} and L_{su} will be qualitative similar to those for B_d. Moreover, the results are given for $n = 10$. This is justified by referring to some of the authors' previous studies (see e.g., Myrhaug and Ong (2011a)). They found that the scour depth and the scour width below pipelines caused by the (1/10)th highest waves represent the upper values of the random wave-induced scour data, and thus suggesting that these values can be used for design purposes. Thus the following example of results for the burial depth will be given for $n = 10$.

Table 2 Example calculation with $h =10$ m , $d_{50} =1$ mm, $h_c =0.5$ m, $(D_b +D_t) /2 =0.75$ m , $n =10$

|	
a_{rms} (m)	1.06
k_p (rad/m)	0.0900
S_1	0.0308
U_R	0.370
α_{2D}, β_{2D} (Eqs. (26 and 27))	0.4017, 1.9467
α_{3D}, β_{3D} (Eqs. (26 and 27))	0.3911, 1.7875
A_{rms}(m)	1.03
U_{rms}(m/s)	0.819
A_{rms} / z_0	12360
c, d, Eq. (8)	0.112, 0.25
KC_{rms}, Eq. (30)	8.6
θ_{rms} , Eqs. (31)	0.220
Burial depth (Eqs. (29) and (34), Table 1)	
B_{dlin} (m)	0.0533
$B_{dnonlin,\ 2D}$ (m)	0.0613
$B_{dnonlin,\ 3D}$ (m)	0.0630
Scour hole width (Eqs. (29) and (34), Table 1)	
$W_{s\ lin}$ (m)	0.990
$W_{s\ nonlin,2D}$ (m)	1.017
$W_{s\ nonlin,3D}$ (m)	1.023
Downstream scour hole length (Eqs. (29) and (34), Table 1)	
$L_{sd\ lin}$ (m)	1.135
$L_{sd\ nonlin\ (2D)}$ (m)	1.212
$L_{sd\ nonlin,\ 3D}$ (m)	1.227
Total scour hole length (Eqs. (29), (34), Table 1)	
$L_{st\ lin}$ (m)	1.520
$L_{st\ nonlin,\ 2D}$ (m)	1.595
$L_{st\ nonlin,\ 3D}$ (m)	1.611
Shields parameter; $\theta_m = \theta_c \cdot \theta_{rms}$	
θ_{clin} , Eq. (40)	2.83
θ_{mlin}	0.623
$\theta_{cnonlin,2D}$, Eq. (39)	3.65
$\theta_{cnonlin,3D}$, Eq. (39)	3.84
$\theta_{m,cnonlin,2D}$	0.803
$\theta_{m,cnonlin,3D}$	0.845
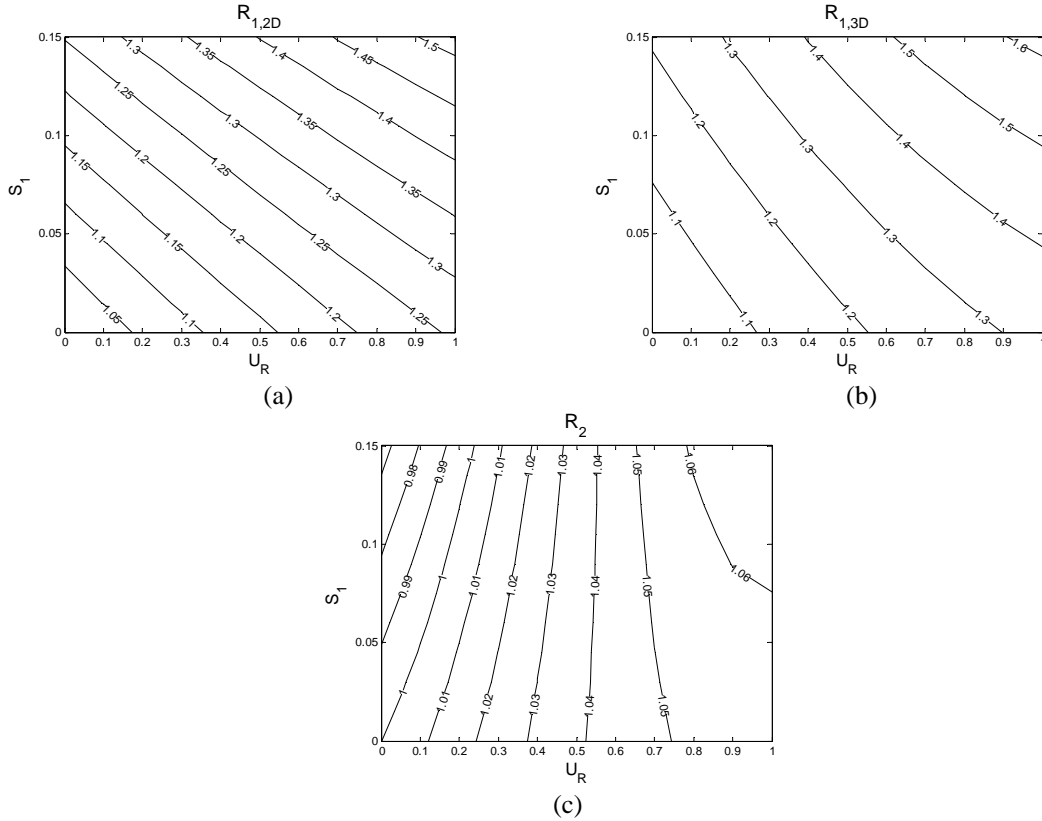
Fig. 2 Isocurves for the ratios R_1 (Eq. (36)) and R_2 (Eq. (37)) for the burial depth B_d versus S_1 and U_R for n = 10, d = 0.25: (a) R_1 for 2D waves, (b) R_1 for 3D waves and (c) R_2. Note that t = 0.975 (Table 1)

Fig. 2 shows the isocurves for the ratios R_1 and R_2 for the burial depth plotted against the wave steepness S_1 and Ursell number U_R. Overall, both for 2D (Fig. 2(a)) and 3D (Fig. 2(b)) waves it appears that: for a given value of U_R, namely at a given water depth, the nonlinear to linear ratio R_1 increases as S_1 increases; for a given value of S_1, R_1 increases as U_R increases (i.e., as the water depth decreases). Those features appears to be physically sound.

Moreover, it appears that R_1 ranges up to about 1.5 for 2D waves (Fig. 2(a)) and up to about 1.6 for 3D waves (Fig. 2(b)). Thus it appears that R_1 is only slightly larger for 3D waves than for 2D waves, except for smaller values of U_R. These features are demonstrated in Fig. 2(c), which shows the isocurves for the 3D results to 2D results ratio, R_2, plotted against S_1 and U_R; except for smaller values of U_R (i.e., for U_R smaller than 0.1 to 0.2 depending on S_1), it appears that the maximum burial depth is always larger beneath 3D waves than beneath 2D waves; R_2 increases as U_R increases (i.e., as the water becomes shallower). This behaviour is caused by the smaller wave setdown effects for short-crested waves than for long-crested waves as mentioned previously in Section 3.1. However, it should be noted that the difference between the results for 2D waves and 3D waves is very small; R_2 ranges up to about 1.06.

4.2 Shields parameter

For random waves it is not obvious which value of the Shields parameter to use to determine the conditions corresponding to live-bed scour. However, it seems to be consistent to use corresponding statistical values of the scour depth and the Shields parameter. That is, if e.g., the value $E\left[Y(w_c)|w_c>w_{c1/n}\right]$ of the scour depth is considered, then the corresponding value of the Shields parameter should be used. Some details of how this value of the Shields parameter for 2D and 3D nonlinear random waves can be calculated will be elaborated in the following.

First, it is noted that the non-dimensional maximum Shields parameter under the wave crest for individual random waves, $\theta_c = \theta_m / \theta_{rms}$, is equal to the non-dimensional maximum bottom shear stress under the wave crest for individual random waves, $\tau_c = \tau_m / \tau_{rms}$. Here θ_{rms} is defined as in Eq. (31) and τ_{rms} is defined as in the denominator in Eq. (31). Moreover, θ_m is defined in Eq. (3) by replacing τ_w with τ_m, i.e., the maximum bottom shear stress under the wave crest for individual random waves. By using this and following Myrhaug and Holmedal (2011), θ_c is given as

$$\theta_c = w_c^{2-d} \tag{38}$$

Then the Shields parameter of interest in the present context is obtained by using the results in the Appendix as

$$E\left[\theta_c(w_c)|w_c>w_{c1/n}\right] = n\left(\sqrt{8}\alpha\right)^{2-d}\Gamma\left(1+\frac{2-d}{\beta},\ln n\right) \tag{39}$$

For linear waves $\left(\alpha = 1/\sqrt{8}, \beta = 2\right)$ the result is

$$E\left[\theta_c(w_c)|w_c>w_{c1/n}\right] = n\Gamma\left(2-\frac{d}{2},\ln n\right) \tag{40}$$

More discussion of the bottom friction beneath 2D and 3D nonlinear random waves are given in Myrhaug and Holmedal (2011).

4.3 Example calculation

This example is included to demonstrate the application of the method. The given flow conditions are:

Significant wave height, $H_s = 3$ m

Spectral peak period, $T_p = 7.9$ s, corresponding to $\omega_p = 0.795$ rad/s

Water depth, $h = 10$ m

Median grain diameter (coarse sand according to Soulsby 1997, Fig. 4) $d_{50} = 1$ mm

$\gamma = 2.65$ (as for quartz sand)

Cone height, $h_c = 0.5\,\mathrm{m}$

Base diameter, $D_b = 1.0$ m

Top diameter, $D_t = 0.5\,\mathrm{m}$

The calculated quantities are given in Table 2. It should be noted that S_1 and U_R are obtained by replacing T_1 and k_1 with T_P and k_P, respectively, since the wave process is assumed to be narrow-banded. The results are exemplified for $n = 10$. Here the *rms* wave amplitude is given according to the Rayleigh distribution by $a_{rms} = H_s / 2\sqrt{2}$. Now A_{rms}/z_0 (i.e., $z_0 = d_{50}/12$) exceeds 11000; thus $(c,d) = (0.112, 0.25)$. Moreover, θ_{rms} exceeds the critical Shields parameter $\theta_{cr} \approx 0.05$, i.e., live-bed conditions.

The maximum equilibrium relative burial depth, the maximum equilibrium scour hole width, the maximum equilibrium downstream scour hole length, and the maximum equilibrium total scour hole length are considered; the effect of nonlinearity is to increase these scour characteristics. The nonlinear to linear ratios for 2D and 3D waves are: 1.15 and 1.18, respectively, for the burial depth; 1.027 and 1.033, respectively, for the scour hole width; 1.068 and 1.081, respectively, for the downstream scour hole length; 1.049 and 1.060, respectively, for the total scour hole length. Consequently, 3D waves give slightly larger values than 2D waves; the 3D to 2D ratios are 1.028 for the burial depth; 1.006 for the scour hole width; 1.012 for the downstream scour hole length; 1.010 for the total scour hole length. It should be noted that these results for the maximum equilibrium relative burial depth, B_d, are consistent with the results in Fig. 2. This is a result of the smaller wave setdown effects for 3D than for 2D waves in finite water depth, as discussed before in the paragraph after Eq. (27).

Finally, for the Shields parameter it is noted that for both linear and nonlinear waves θ_m exceeds θ_{cr} implying live-bed conditions. Short-crested waves give a slightly larger value than long-crested waves.

4.4 Discussion

Catano-Lopera *et al*. (2011) discussed several issues regarding how the sediment properties and the presence of ripples in the vicinity of the scour hole around the truncated cone influence the scour characteristics; see their paper for more details.

Experimental errors were also addressed. In particular, the experimental error plays an important role in the validity of Eq. (1), "implying that the use of Eq. (1) should be made with caution".

Scale effects associated with such as bedform size, cone size, sediment size, water depth and time-dependent burial depth were also discussed. However, overall the results indicate no significant scale effects. But as stated by Catano-Lopera *et al*. (2011): "Nevertheless, the use of any of the empirical relations developed in the study should be exercised with caution". This statement is still valid when using the results based on the present stochastic method.

Although simple, the present approach should be useful as a first approximation to represent the stochastic properties of the maximum equilibrium scour characteristics around truncated cones exposed to random waves. However, comparisons with data are required before a conclusion regarding the validity of this approach can be given. In the meantime the method should be useful as an engineering tool for design purposes.

5. Conclusions

A practical stochastic approach for estimating the maximum equilibrium scour characteristics around truncated cones due to long-crested (2D) and short-crested (3D) nonlinear random waves is given.

An example calculation demonstrates the effects of nonlinear waves. The scour characteristics are only slightly larger beneath 3D nonlinear waves than beneath 2D nonlinear waves. This behaviour is attributed to the smaller wave setdown effects for 3D than for 2D waves in finite water depth.

Although simple, the present approach should be useful as a first approximation to represent the stochastic properties of the maximum equilibrium scour characteristics around truncated cones exposed to 2D and 3D nonlinear random waves. However, comparisons with data are required before a conclusion regarding the validity of this approach can be given. In the meantime the method should be useful as an engineering tool for the assessment of scour and in scour protection work.

References

Abramowitz, M. and Stegun, I.A. (1972), *Handbook of mathematical functions*, Dover, New York.

Catano-Lopera, Y.A. and Garcia, M.H. (2007), "Geometry of scour hole around, and the influence of the angle of attack on the burial of finite length cylinders under combined flows", *Ocean Eng.*, **34**(5-6), 856-869.

Catano-Lopera, Y.A., Landry, B.J. and Garcia, M.H. (2011), "Scour and burial mechanics of conical frustums on a sandy bed under combined flow conditions", *Ocean Eng.*, **38**, 1256-1268.

Dean, R.G. and Dalrymple, R.A. (1984), *Water wave mechanics for engineers and scientists*, Prentice-Hall, Inc., New Jersey, USA.

Forristall, G.Z. (2000), "Wave crest distributions: Observations and second-order theory", *J. Phys. Oceanogr.*, **30**, 1931-1943.

Guyonic, S., Mory, M., Wever, T.F., Ardhuin, F. and Garland, T. (2007), "Full-scale mine burial experiments in wave and current environments and comparison with models", *IEEE J. Oceanic Eng.*, **32**(1), 119-132.

Jenkins, S.A., Inman, D.L., Richardson, M.D., Wever, T.F. and Wasyl, J. (2007), "Scour and burial mechanics of objects in the nearshore", *IEEE J. Oceanic Eng.*, **32**(1), 78-90.

Mayer, L.A., Raymond, R., Clang, G., Richardson, M.D., Traykovski, P. and Trembanis, A.C. (2007), "High-resolution mapping of mines and ripples at the Martha's Vineyard coastal observatory", *IEEE J. Oceanic Eng.*, **32**(1), 133-149.

Myrhaug, D. and Holmedal, L.E. (2011), "Bottom friction and erosion beneath long-crested and short-crested nonlinear random waves", *Ocean Eng.*, **38**(17-18), 2015-2022.

Myrhaug, D., Holmedal, L.E., Simons, R.R. and MacIver, R.D. (2001), "Bottom friction in random waves plus current flow", *Coast. Eng.*, **43**(2), 75-92.

Myrhaug, D. and Ong M.C. (2011a), *Random wave-induced scour around marine structures using a stochastic method. in: marine technology and engineering*, (Eds., C. Guedes Soares *et al.*), CRC Press/Balkema,Taylor & Francis Group, London, UK.

Myrhaug, D. and Ong, M.C. (2011b), "Long- and short-crested random wave-induced scour below pipelines", *P. I. Civil Eng. - Mar. En.*, **164**(4), 173-184.

Myrhaug, D. and Ong, M.C. (2012), "Scour around spherical bodies due to long-crested and short-crested nonlinear random waves", *Ocean Syst. Eng.*, **2**(4), 257-269.

Myrhaug, D. and Ong M.C. (2013a), "Scour around vertical pile foundations for offshore wind turbines due to long-crested and short-crested nonlinear random waves", *J. Offshore Mech. Arct.*, **135**(1), 011103.

Myrhaug, D. and Ong, M.C. (2013b), "Effects of sand-clay mixtures on scour around vertical piles due to long-crested and short-crested nonlinear random waves", *J. Offshore Mech. Arct*, **135**(3), 034502.

Myrhaug, D., Ong, M.C., Føien, H., Gjengedal, C. and Leira, B.J. (2009), "Scour below pipelines and around vertical piles due to second-order random waves plus a current", *Ocean Eng.*, **36**(8), 605-616.

Myrhaug, D., Ong, M.C. and Hesten, P. (2012), "Burial and scour of short cylinders due to long-crested and short-crested nonlinear random waves", *Proceedings of the 6th Int. Conf. on Scour and Erosion*, Paris, France, August 27-31.

Ong, M.C., Myrhaug, D. and Hesten, P. (2013), "Scour around vertical piles due to long-crested and short-crested nonlinear random waves plus a current", *Coast. Eng.*, **73**, 106-114.

Sharma, J.N. and Dean, R.G. (1981), "Second-order directional seas and associated wave forces", *Soc. Petrol. Eng. J.*, **21**, 129-140.

Soulsby, R.L. (1997), *Dynamics of marine sands. a manual for practical applications*, Thomas Telford, London, UK.

Sumer, B.M. and Fredsøe, J. (1996), "Scour below pipelines in combined waves and current", *Proceedings of the15th OMAE Conf.*, Florence, Italy.

Sumer, B.M. and Fredsøe, J. (2001), "Scour around pile in combined waves and current", *J. Hydraul. Eng. - ASCE*, **127**(5), 403-411.

Sumer, B.M. and Fredsøe, J. (2002), *The mechanics of scour in the marine environment*, World Scientific, Singapore.

Whitehouse, R.J.S. (1998), *Scour at marine structures*, A Manual for Practical Applications, Thomas Telford, London, UK.

Appendix

Let *x* be Weibull distributed with the *pdf*

$$p(x) = \beta x^{\beta-1} \exp(-x^\beta); \ x \geq 0, \beta > 0 \tag{A1}$$

The expected value of the $(1/n)$th   largest values of *x* is given as

$$E[x_{1/n}] = n \int_{x_{1/n}}^\infty xp(x)\,dx \tag{A2}$$

where $x_{1/n}$ is the value of   *x* which is exceeded by the probability $1/n$.

Moreover, from Abramowitz and Stegun (1972, Ch. 6.5, Eq. (6.5.3)) it is given that

$$\Gamma(a,x) = \int_x^\infty e^{-t} t^{a-1}\,dt \tag{A3}$$

By utilizing this, the following result is obtained

$$\int_{x_1}^\infty x^m p(x)\,dx = \int_{x_1}^\infty x^m \beta x^{\beta-1} \exp(-x^\beta)\,dx = \Gamma\left(1 + \frac{m}{\beta}, x_1^\beta\right) \tag{A4}$$

by using Eq. (A1), and   where $\Gamma(\Box,\Box)$ is the   incomplete gamma function: $\Gamma(x,0) = \Gamma(x)$ where Γ is the gamma function. The result in Eq. (A4) is obtained by substituting $t = x^\beta$ in the second integral in Eq. (A4) and using Eq. (A3).